



Superparamagnetic iron oxide nanoparticles exert different cytotoxic effects on cells grown in monolayer cell culture versus as multicellular spheroids



Anja Theumer^{a,1}, Christine Gräfe^{a,1}, Franziska Bähring^a, Christian Bergemann^b,
Andreas Hochhaus^a, Joachim H. Clement^{a,*}

^a Department of Hematology and Oncology, Jena University Hospital, Erlanger Allee 101, 07747 Jena, Germany

^b Chemicell GmbH, Eresburgstrasse 22–23, 12103 Berlin, Germany

ARTICLE INFO

Article history:

Received 30 June 2014

Received in revised form

9 October 2014

Accepted 13 October 2014

Available online 18 October 2014

Keywords:

Cytotoxicity

3D

Akt signalling

SPIO

ABSTRACT

The aim of this study was to investigate the interaction of superparamagnetic iron oxide nanoparticles (SPIO) with human blood–brain barrier-forming endothelial cells (HBMEC) in two-dimensional cell monolayers as well as in three-dimensional multicellular spheroids. The precise nanoparticle localisation and the influence of the NP on the cellular viability and the intracellular Akt signalling were studied in detail. Long-term effects of different polymer-coated nanoparticles (neutral fluidMAG-D, anionic fluidMAG-CMX and cationic fluidMAG-PEI) and the corresponding free polymers on cellular viability of HBMEC were investigated by real time cell analysis studies. Nanoparticles exert distinct effects on HBMEC depending on the nanoparticles' surface charge and concentration, duration of incubation and cellular context. The most severe effects were caused by PEI-coated nanoparticles. Concentrations above 25 µg/ml led to increased amounts of dead cells in monolayer culture as well as in multicellular spheroids. On the level of intracellular signalling, context-dependent differences were observed. Monolayer cultures responded on nanoparticle incubation with an increase in Akt phosphorylation whereas spheroids on the whole show a decreased Akt activity. This might be due to the differential penetration and distribution of PEI-coated nanoparticles.

© 2015 Elsevier B.V. All rights reserved.

1. Introduction

Based on their unique and versatile features, nanomaterials attract widespread interest in both research and industry. In the biomedical field especially magnetic multifunctional nanoparticles (NP) composed of iron oxide cores have various applications in magnet resonance imaging, drug delivery, and hyperthermal anti-tumour therapy [1–3]. Whereas several iron oxide-based NP are already clinically approved as contrast agents [4], their real biological effect on distinct tissues or individual cells remains unclear. Previous studies have mostly focused on NP biocompatibility within the sense of cytotoxicity [5,6], while their effects on normal cell physiology and signal transduction of human tissue cells inevitably exposed NP upon biomedical application, remain widely unknown [7,8].

Based on their large surface to volume ratio, NP play a special role concerning reactivity and interaction with matrices. These particles may not only be capable of passive interaction with cells and cellular membranes, but may also interfere directly with various membrane receptors, thereby affecting and modulating signalling transduction pathways [9]. The membrane receptor-activated protein Akt, also referred to as protein kinase B (PKB), is a central element within the cellular signalling network [10].

This protein kinase plays a critical role in vital cellular processes, including survival, proliferation, and metabolism. Activated Akt promotes cell survival and inhibits the induction of programmed cell death, also called apoptosis. Thus, pro-apoptotic proteins like caspase-9, Bad, and forkhead transcription factors are inhibited upon Akt phosphorylation, whereas inhibitors of apoptosis such as Birc5, also known as survivin, are stimulated.

However, testing the toxicity of nanoparticles or their influence on cellular signalling in monolayers may deviate from the adequate biological effect *in vivo* due to their loss of tissue-specific properties [11]. Thus, two-dimensional cell cultures show differences in transport conditions and the absence of distinct cell–cell or cell–matrix interactions, respectively, so that contradictory

* Corresponding author. Fax: +49 3641 9325822.

E-mail address: joachim.clement@med.uni-jena.de (J.H. Clement).

¹ Both authors contributed equally to this work.

results of toxicity studies were achieved between monolayers and *in vivo* animal models [12].

One option to bridge the gap between these two models is the application of multicellular spheroids which represent an *in vitro* 3D cell culture that consists of assembled spherical-arranged cell colonies [13]. These closely packed structures model the physiological 3D architecture of tissues, since they possess a strongly deposited extracellular matrix and biochemical gradients which influence gradient-dependent cellular responses [14]. The extracellular matrix provides cell–matrix interactions and the linking of secreted chemokines, growth factors, and a variety of signalling proteins in matrix-binding forms [14,15]. Another advantage of 3D cultures compared to monolayers is the presence of pronounced intracellular junctions mimicking physiological barriers [16]. These cellular junctions as well as the dense extracellular matrix with small pores affect the transport of drugs, nanoparticles and other compounds by reducing their penetration [12,13,17]. Therefore multicellular spheroids are also suitable as a model to test drug delivery or to investigate the toxicity and the infiltration of nanoparticles through physiological barriers [15].

As the human blood–brain barrier is a critical and sensitive interface necessarily exposed to systemically applied NP, we investigated the NP-induced effect on the cellular viability and the central Akt signalling of human blood–brain barrier-forming cells. For this purpose two distinct *in vitro* cell culture models were established: on the one hand a blood–brain barrier-representing two-dimensional cell monolayer of human brain microvascular endothelial cells (HBMEC) and on the other hand a more complex three-dimensional multicellular spheroidal system composed of HBMEC.

Based on previous literature apart from particles' material composition, size, and shape especially the NP surface charge plays a pivotal role in determining the particular interaction with biological systems as well as their cellular uptake [18–21]. That is why in this study expediently, analysed spherical NPs of similar size were chosen according to their surface charge resulting from different polymer coatings: neutral starch-coated (fluidMAG-D), cationic polyethylenimine-coated (fluidMAG-PEI), and anionic carboxymethyl dextran-coated (fluidMAG-CMX) iron oxide cored NP. Results show a concentration-dependent cytotoxic effect of cationic fluidMAG-PEI in both 2D and 3D cellular systems. Regarding Akt signalling pathway analysis a strong global Akt activation is found in cell monolayers especially for the cationic NP, whereas investigations in 3D spheroids reveal deviating outcomes, which might be substantiated in time-dependent spatial distributions and indicating a context-dependant effect of NPs on cellular processes.

2. Experimental methods

All chemicals were purchased by Sigma-Aldrich (Taufkirchen, Germany) or Life technologies (Darmstadt, Germany) if not otherwise stated.

2.1. Cell culture

Human brain microvascular endothelial cells (HBMEC) represent a reasonable and widely used *in vitro* cell culture model of the human blood–brain barrier. The cell line immortalised by the introduction of the SV40 large T antigen [22], was cultured at 37 °C and 5% CO₂ in RPMI 1640 medium supplemented with GlutaMAX™ and 10% foetal calf serum (Biochrom-Seromed, Berlin, Germany) in a humidified atmosphere. Cell cultures with 90% confluency were split in ratios between 1:8 and 1:12 and supplied with fresh medium. Cell cultures were used up to passage 30.

Multicellular spheroids were created with the hanging-drop method [23]. Medium drops with a volume of 20 µl containing 20,000–30,000 cells were disseminated on a petri dish lid (28.3 cm²) and the lid was turned upside down. Due to gravity multicellular spheroids formed at the bottom of each drop within 4–5 days in an incubator at 37 °C in a humidified atmosphere with 5% CO₂.

2.2. Nanoparticles and free polymers

All nanoparticles were provided by Chemicell GmbH, Berlin. They possessed a core made of iron oxide and a shell of differently charged polymers. According to the manufacturer's specifications the hydrodynamic diameters of neutral starch-coated fluidMAG-D, cationic polyethylenimine (PEI, MW = 750 kDa)-coated fluidMAG-PEI, and anionic carboxymethyl dextran (CMX)-coated fluidMAG-CMX nanoparticles were 150 nm, 100 nm, and 150 nm, respectively. The hydrodynamic diameters of the fluorochrome-labelled nano-screen MAG/G-D, nano-screen MAG/G-PEI and nano-screen MAG/G-CMX were 150 nm. The cores are additionally covered with a lipophilic dye (ex = 476 nm, em = 490 nm).

2.3. Real time cell analysis

The viability of incubated HBMEC was monitored via real time cell analysis (RTCA) using the xCELLigence system by Roche Applied Science (Mannheim, Germany). This non-invasive approach is based on electronic impedance measurements accomplished by gold microelectrode sensor arrays integrated into each bottom of 16 well E plates. As cells altering the local ion environment and adhering to the electrode-covered surface, act as insulators, relative changes in the measured impedance can be associated with variations in cell number, morphology, degree of adhesion, and cellular viability represented by the dimensionless parameter cell index (CI). Thus, rising numbers of vital cells are accompanied by increasing impedance values, whereas decreasing impedances are associated with cytotoxic events [24].

64,000 cells/cm² were seeded in a well of a 16 well E plate, each. After a 30-min sedimentation period cells were monitored in real time at 37 °C in a humidified atmosphere with 5% CO₂. Following 24 h of cultivation the compounds were added to the cells and mixed carefully before RTCA was continued for up to 72 h. Medium-treated cells and cell-free compound-treated wells served as controls.

2.4. Cell lysis and immunoblotting

HBMEC monolayers cultured in 6-well plates (64,000 cells/cm², Greiner Bio-One, Frickenhausen, Germany) or a pool of 90 spheres incubated with respective compounds for indicated durations were washed twice with *ν*-PBS, harvested, and lysed in 20 mM HEPES, 150 mM NaCl, 10 mM EDTA (pH 8.0), 2 mM EGTA (pH 8.0), 1% (v/v) Triton X 100, 10 mM Na₄P₂O₇, 50 mM NaF, 2 mM Na₃VO₄ supplemented with aprotinin (10 µg/ml), pepstatin (1 µM), leupeptin (10 µM), and PefaBloc (500 µg/ml). After a centrifugation step (20 min at 16,200g, 4 °C) total protein was quantified using the Bradford method [25]. Proteins were separated by SDS-PAGE (4–12% Criterion™ XT precast gel, BioRad) and transferred to Immobilon membranes (BioRad Laboratories, Munich, Germany). Immobilised proteins were multistrip-probed with 1000-fold diluted specific antibodies against phospho-Akt (Ser473) and pan-Akt (Cell Signaling Technologies, Heidelberg, Germany). Staining with actin (α,β,γ)-directed antibodies (1:5000 dilution, Santa Cruz Biotechnology, Heidelberg, Germany) served as loading control.

2.5. Staining of cells and confocal microscopy

For microscopic analysis HBMEC cells were seeded on glass cover slips (12 mm diameter, Menzel, Braunschweig, Germany) in 24-well tissue culture plates (76,000 cells/cm², Greiner Bio-One). 3D-scaled spheres of HBMEC were transferred to black-walled 96-well glass plates (Greiner Bio-One). Cells were incubated with respective nanoparticle- or polymer formulations. The effects of iron oxide NP onto the viability of these cells were examined by determining the ratio of living cells to dead cells using the LIVE/DEAD[®] Viability/Cytotoxicity Kit which includes two dyes, calcein (excitation: 494 nm, emission: 517 nm) and ethidium homodimer-1 (excitation: 528 nm, emission 617 nm).

For analysing NP uptake into both HBMEC monolayers and spheroidal cell systems, cells were incubated with fluorochrome-labelled NP for 3 h. Then, cells were washed three times with D-PBS, fixed with 4% (w/v) paraformaldehyde (10 min), and permeabilized using 0.1% (v/v) Triton X 100 (10 min). Cytoskeletal F-actin and nuclei were stained with Alexa Fluor 633 phalloidin (1:66) and DAPI II (1:100, Abbott Laboratories, Wiesbaden, Germany), respectively.

Fluorescence was measured using the confocal laser scanning microscope LSM 510 META (Carl Zeiss Microscopy GmbH, Jena, Germany). Images of relative fluorescence intensity [AU] were created with MATLAB (MathWorks, Natick, USA).

2.6. Statistical analysis

Mean values obtained from repeated, independent experiments were statistically analysed using the one-way ANOVA combined with multiple comparison (MATLAB, MathWorks), where *p*-values

< 0.05 were considered as statistically significant. Quantile–quantile plots validated normal distribution of measured data.

3. Results and discussion

3.1. Nanoparticle-associated cytotoxicity

Cytotoxic effects of iron oxide nanoparticles on cells are highly connected to the particle surface charge predominantly provoked by the nanoparticles' coating material. We could previously show that both neutral and anionically charged NP generally do not compromise cell viability, but identical concentrations of cationic NP have severe cytotoxic effects even after 3 h of exposure [5]. Based on these results long-term effects of differently charged NP on HBMEC were evaluated by real-time cell analysis. Cationic PEI-coated NP affect HBMEC monolayers in a concentration-dependent manner. Starting with 25 µg/cm² the PEI-coated NP exhibit a harmful effect on the cells (Fig. 1A). 100 µg/cm² of the cationic NP lead to a dramatic impairment of cellular viability being most pronounced between 12 and 24 h after compound addition (Fig. 1). During prolonged incubation cell cultures recover from the inhibitory conditions. After 50 h of treatment with PEI-coated NP HBMEC cell cultures reach similar cell indices like the medium-treated control cells. In contrast application of 100 µg/cm² of both neutral and anionic fluidMAG-D and -CMX do not affect cell viability at all. Dürr et al. could show previously that real-time cell analysis is a suitable tool to study long-term effects of pharmaceutical drugs coupled to nanomaterials on tumour cell lines with the focus on the drug-dependent reaction of the cells [26].

Our results show that even in the presence of cytotoxic NP a subpopulation of the affected cell culture is able to survive. Beside

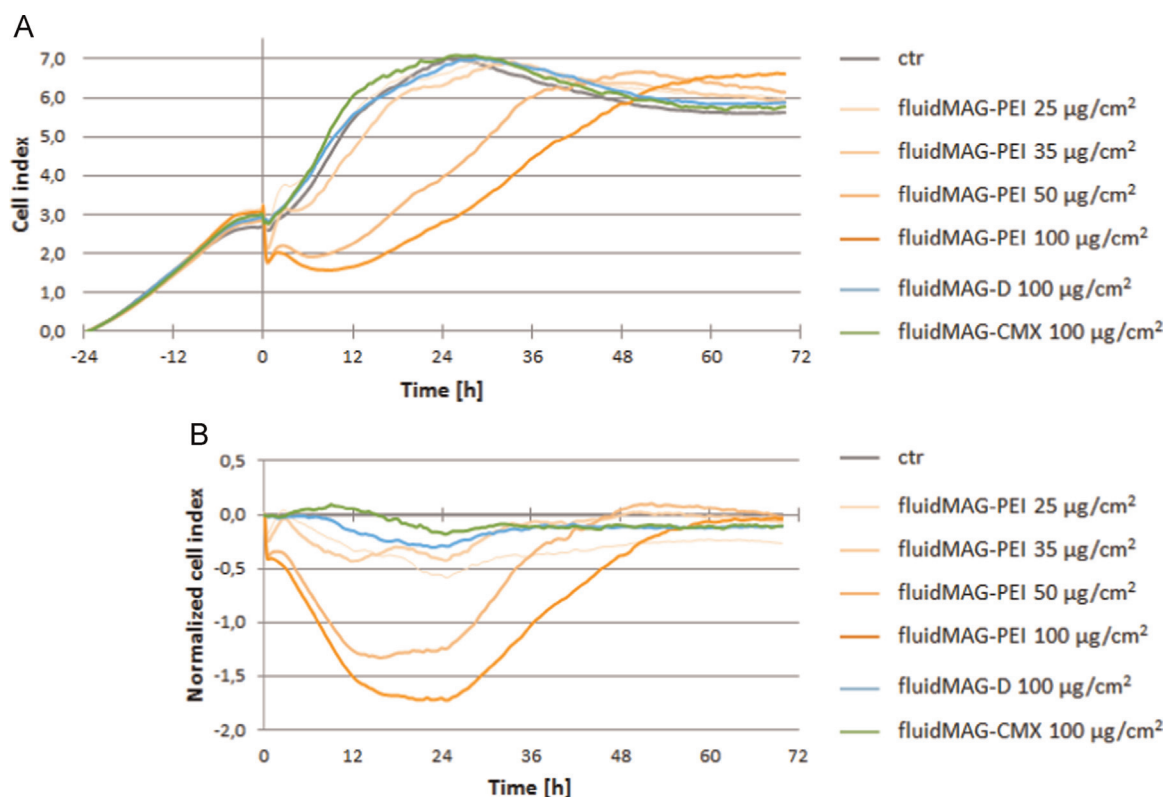


Fig. 1. Long-term monitoring of cytotoxic effects of NP. HBMEC were seeded into 16 well E plates (64,000 cells/cm²) and cultured for 24 h prior to treatment. At *t*=0 h indicated concentrations of NP formulations or medium (ctr) were added. Cell viability was monitored for further 72 h. (A) Mean of absolute real-time cell indices obtained during the entire experiment. (B) Data were normalised to the time point when compounds were added and additionally subtracted by the respective data obtained from medium-treated control cells. Values represent means of two technical replicates.

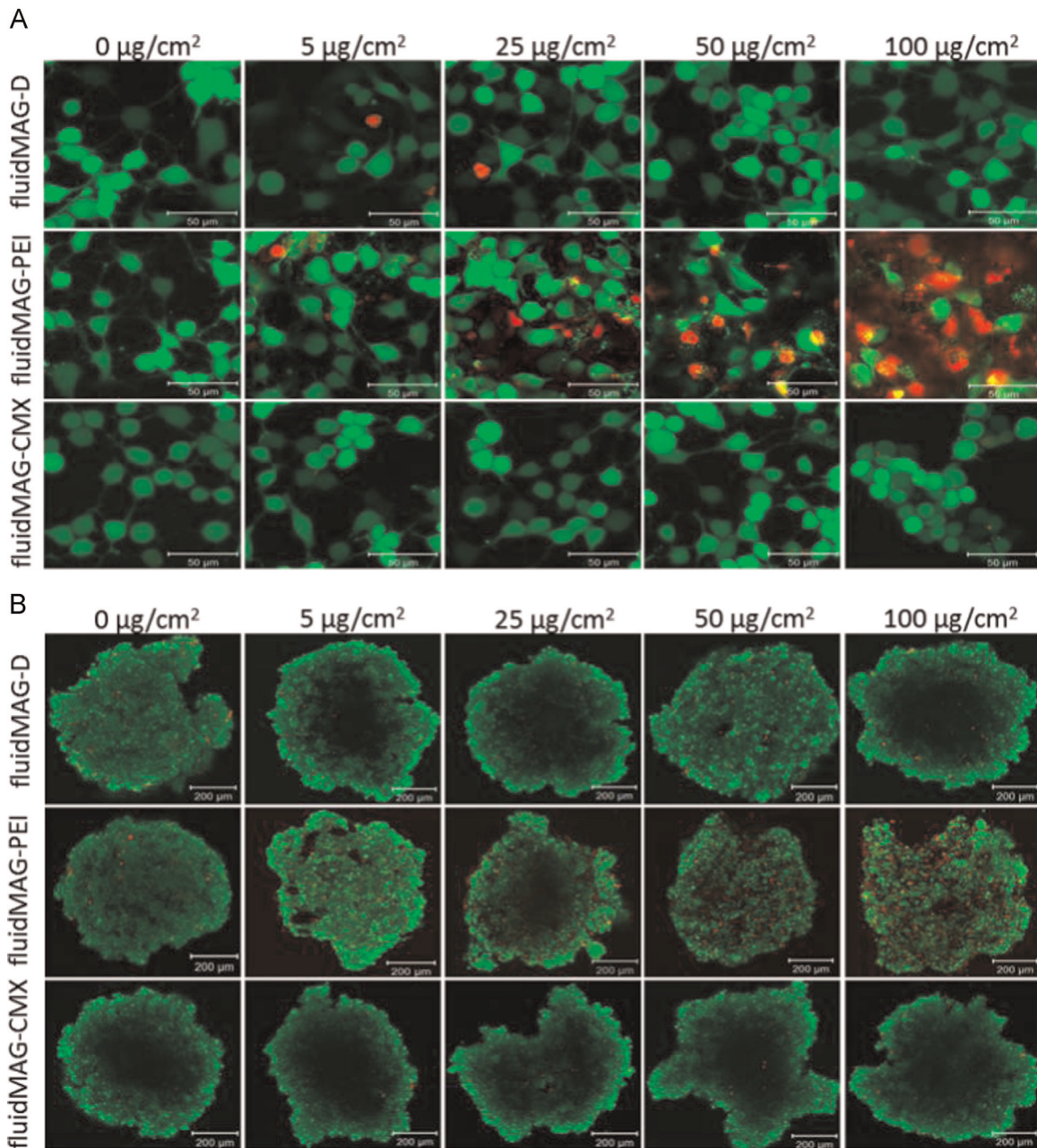


Fig. 2. PEI-coated nanoparticles cause severe cell damage in 2D and 3D cell culture. HBMEC monolayers were seeded on cover slips in 24-well culture plates with a density of 76,000 cells/cm². The following day monolayers (A) and spheroids (B) were treated with fluidMAG-D, fluidMAG-PEI and fluidMAG-CMX in indicated concentrations for 3 h. Live/dead staining was performed with the LIVE/DEAD[®] Viability/Cytotoxicity Kit and cell viability was investigated with confocal laser scanning microscopy. Viable cells are shown in green, dead cells are represented in red. Pictures of HBMEC monolayers were recorded with a magnification of 630 ×, images of spheroids are magnified 100-fold. Scale bars indicate 50 µm (A) and 200 µm (B). (For interpretation of the references to colour in this figure legend, the reader is referred to the web version of this article.)

the concentration and the time of duration the arrangement of the cells might contribute to this observation. In contrast to a monolayer cell culture the organisation of cells in organs is 3-dimensional. Therefore we established HBMEC cell cultures in multicellular spheroids and investigated their interaction behaviour with differentially charged NP compared to 2-dimensional HBMEC cultures. At first HBMEC monolayers and spheroids were studied by fluorescence-based live/dead staining after incubation with fluidMAG-D, fluidMAG-PEI and fluidMAG-CMX with the indicated concentrations for 3 h. The microscopic analysis show that neutral fluidMAG-D as well as anionic fluidMAG-CMX NP do not affect the viability of HBMEC in monolayers (Fig. 2A) as well as in spheroids (Fig. 2B). The ratio of viable to dead cells remains constant even with increasing particle concentrations. In contrast, the live/dead

staining of both monolayers (2D) as well as spheroids (3D) confirms an increased amount of red-stained cells, *i.e.* dead cells after incubation with cationic particles. FluidMAG-PEI exhibits concentration-dependent cytotoxic effects starting with 25 µg/cm². The dramatic reduction in cellular viability after treatment with high concentrations of fluidMAG-PEI NP is demonstrated by an increased portion of dead cells and the subsequent shift in the ratio of viable to dead cells. Please note, the amount of dead cells is more pronounced in the 2D cell cultures compared to spheroids. However, no cytotoxic effects are observed after incubation of cells with 5 µg/cm² PEI. The same results for both monolayers and multicellular spheroids were achieved after incubation with the corresponding free polymers (data not shown).

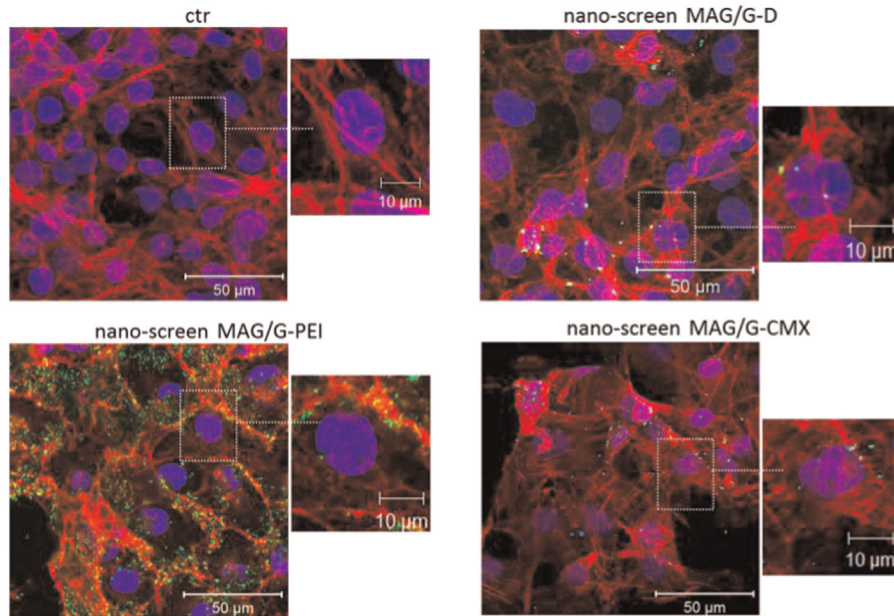


Fig. 3. Charge-dependant distribution of NP in 2D cell cultures. HBMEC monolayers were seeded on glass cover slips in 4-well culture plates with a density of 76,000 cells/cm² and cultured overnight. Cells were treated with fluorochrome-labelled nano-screen MAG/G-D, nano-screen MAG/G-PEI and nano-screen MAG/G-CMX (green) in a concentration of 25 µg/cm² for 3 h. Cytoskeletal F-actin of fixed and permeabilized cells was stained with phalloidin-Alexa Fluor 633 (red) and nuclei were visualised with DAPI (blue). NP localisation was investigated by confocal laser scanning microscopy. Pictures of HBMEC monolayers were recorded with a magnification of 630 ×. (For interpretation of the references to colour in this figure legend, the reader is referred to the web version of this article.)

3.2. Nanoparticle uptake and spatial distribution

Next, we were interested to study the uptake, penetration, and distribution of the differentially charged NP into cells in monolayer culture *versus* multicellular spheroids. In comparison to the non-labelled fluidMAG-nanoparticles the magnetic core of the fluorochrome-labelled NP is additionally covered by a green lipophilic dye (ex=476 nm, em=490 nm). Due to the less pronounced PEI-associated cytotoxic effect at lower concentrations, HBMEC

monolayers on cover slips as well as spheroids were incubated with nano-screen MAG/G-D, nano-screen MAG/G-PEI and nano-screen MAG/G-CMX particles with a concentration of 25 µg/cm² for 3 h. Incubated cells were counterstained with phalloidin-Alexa Fluor 633 and DAPI to visualise the actin cytoskeleton and the nucleus, respectively. NP distribution was analysed by laser scanning microscopy. Each photomicrograph represents a projection of several levels (z-stack). In the 2-dimensional monolayer setting, NP are distributed more or less equally over the cell layer

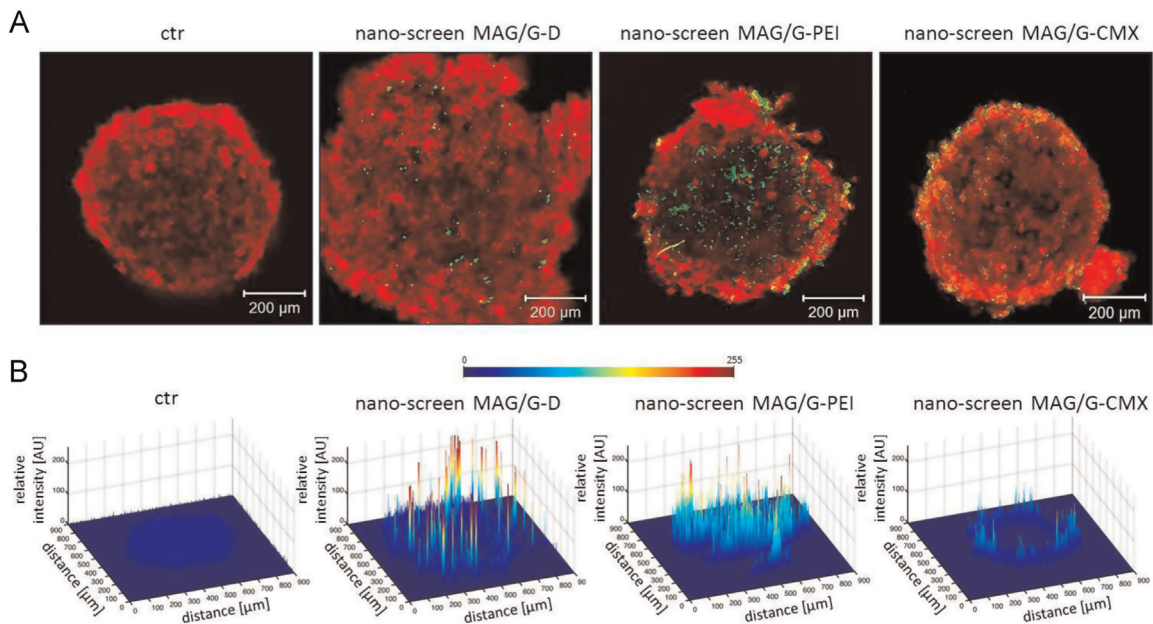


Fig. 4. Spatial nanoparticle distribution in HBMEC spheroids. Spheroids were treated with nano-screen MAG/G-D, nano-screen MAG/G-PEI and nano-screen MAG/G-CMX (green) in a concentration of 25 µg/cm² for 3 h. F-actin of fixed and permeabilized cells was stained using Alexa Fluor 633 phalloidin (red). NP distribution was analysed by confocal laser scanning microscopy. (A) 3D overlays of spheroids' z-stacks recorded at a magnification of 100 ×. Scale bars indicate 200 µm. (B) Relative fluorescence intensity of labelled NP was plotted according to their spatial location within the middle cross section of the spheroid. Dark blue colour indicates no fluorescence, red colour indicates high fluorescence. (For interpretation of the references to colour in this figure legend, the reader is referred to the web version of this article.)

independent of charge (Fig. 3). All three NP types are taken up into the cells. Internalised NP are located within the cytoplasm but not within the nucleus. Strikingly, particle surface charge seems to determine the frequency of NP uptake. PEI-coated NP are preferentially located at the outer side of the cell membrane in contrast to starch- or CMX-coated nanoparticles.

In multicellular spheroids nanoparticles exert charge-dependant distribution patterns. Cationic as well as neutral charged particles penetrate the whole spheroid within the 3 h incubation period, whereas anionic nano-screen MAG/G-CMX nanoparticles remain preferentially in the outer cell layer (Fig. 4A). Cationic nanoparticles form clusters throughout the spheroids, whereas neutral-charged nanoparticles form few clusters randomly distributed within the spheroids. The characteristic charge-dependant localisation of the nanoparticles is highlighted when plotting NPs' relative fluorescence intensity versus their spatial location within the middle cross section of the spheroids (Fig. 4B).

The distribution of the NP is a dynamic time- and charge-dependent process. Even 5 min after NP application nano-screen MAG/G-PEI are already found within the whole spheroid. In contrast, nano-screen MAG/G-D nanoparticles need at least 30 min to reach the spheroidal centre (data not shown). After a 3 h incubation nanoparticles could be detected within cells of the spheroids independent to their charge.

The NP-specific distribution pattern in spheroids may not only depend on the charge but may also be affected by other features. On the one hand, characteristics of the multicellular spheroids, e.g. an extensive extracellular matrix with critical pore sizes or the tortuosity of the interstitial space contribute to NP-spheroid interaction [17]. Thus, NP with a diameter below 100 nm seem to

penetrate spheroids more easily [13,27]. Therefore, the distribution of the anionic NP in the peripheral rim of the spheroid might be at least in part explained by the average diameter of 150 nm which hampers the passage through the extracellular matrix. In contrast, the localisation of cationic and neutral NP within the spheroids might be facilitated by their size of 100 nm and 150 nm, respectively.

3.3. Nanoparticles' effect on Akt signalling

The previous investigations show that the NP-cell interaction depends on the charge and on the context of the cells (2D versus 3D cell culture). The resulting cellular responses are triggered by changes in intracellular signalling. An important signalling pathway involved in various cellular processes, e.g. proliferation or cell survival, is the PI3K/Akt/mTOR pathway. We analysed the activity of a key player, the Akt tyrosine kinase, in dependence of the differentially charged nanoparticles. Furthermore we take the incubation time and the cellular context into account. Representative Western blot analyses are shown in Fig. 5A.

Incubation of HBMEC monolayer cultures shows a slight activation of Akt after incubation with fluidMAG-D and -CMX. Although no statistical differences were detectable after any particle treatment, PEI-coated NP exhibit the most considerable effect. The amount of phospho-Akt is increased 2-fold compared to control cells after 30 min of incubation (Fig. 5B). However, in the 3D cell culture system the application of the NP causes quite different results. The Akt signal is attenuated after 5 min of incubation with fluidMAG-D, followed by an increase of protein content and a sharp decline after 180 min (Fig. 5C). Phospho-Akt levels of

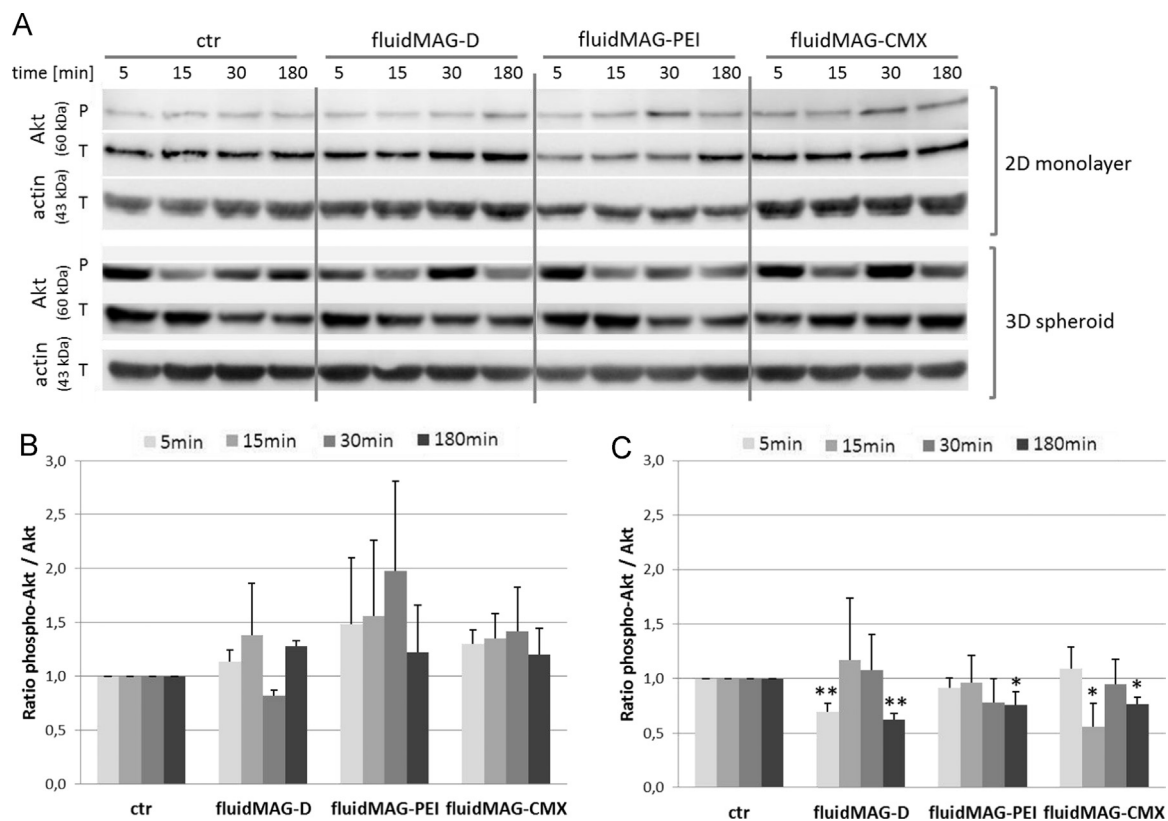


Fig. 5. Nanoparticle cell interaction affects intracellular Akt signalling. HBMEC monolayers or a pool of 90 spheres per sample were incubated with fluidMAG-D, fluidMAG-PEI and fluidMAG-CMX in a concentration of $25 \mu\text{g}/\text{cm}^2$ for indicated times. Proteins from cellular lysates were separated by SDS-PAGE and immunodetected using antibodies binding phosphorylated or total amounts of Akt. Binding of actin served as a loading control. (A) Representative blots from 2D and 3D cell culture obtained from three independent incubation experiments. Optical densities of bands achieved from Western blot analysis of monolayers (B) and spheroids (C) were quantified using the ImageJ software. Data are expressed as ratios of phospho-Akt (Ser473) to total Akt, whereby samples were normalised to respective medium-treated control samples which were set 100%. Data are expressed as % of control mean \pm SEM of three independent experiments. * $p < 0.05$, ** $p < 0.01$. P-phosphorylated protein; T-total protein.

spheroids exposed to fluidMAG-CMX are not significantly altered after 5 and 30 min of incubation, but indicate a decline after 180 min. Finally, PEI-coated NP led to a continuous decrease of the Akt signal in three-dimensional cell cultures which might be in part due to the changes in total Akt protein content. This is in clear contrast to the results with the 2D cell culture system.

The observation that cells grown in 2D and 3D cell culture exhibit differences in response to external stimuli are also described in toxicology studies, e.g. the application of siRNA constructs via PEGylated polyplexes [27,28]. The more or less uniform distribution of the NP in 2D and the clear allocations in 3D might be responsible for the differences in cellular responses, including Akt activation. Rauch et al. described a comparable time course of Akt activation in transformed cell lines from breast epithelium and colon after iron oxide nanoparticle application indicating that HBMEC are a suitable endothelial model for further NP studies [8]. Apart from these possible size-dependent effects of NP penetration into cellular spheroids the particles' charge itself might also play an essential role. Microscopic investigations of NP uptake into 2D HBMEC monolayers clearly indicate a strongly reduced interaction and internalisation of anionic fluidMAG-CMX compared to both neutral starch- and cationic PEI-coated NP, which corresponds to similar charge-associated internalisation rates observed by other groups [18,20]. Thus, these effects might contribute to a diminished penetration of anionic NP into the 3D cell structures as well.

In conclusion we could demonstrate that two-dimensional cell monolayers as well as three-dimensional multicellular spheroids are suitable models to investigate the interaction of endothelial cells with SPIONs. Both cell culture-based systems allow studies on the localisation of the nanoparticles and on the resulting vitality of the cells with respect to the charge of the nanoparticles. The observed context-dependant variations in the activity of intracellular Akt signalling in response to the application of differentially charged nanoparticles need further investigation. Ongoing research concentrates on downstream targets of Akt signalling as well as on other important intracellular signalling pathways. Furthermore the role of the size of the applied nanoparticles in concert with the overall charge will be an important issue of upcoming investigations.

Acknowledgement

The technical assistance of Cornelia Jörke is highly acknowledged. This work was supported in part by the German Federal Ministry of Education and Research under Research Program "NanoCare": Toxicological characterization of nanomaterials for diagnostic imaging in medicine (NanoMed) (Grant 03 × 0104D) and the Deutsche Forschungsgemeinschaft Priority Program 1681 (Grant CL202/3-1)

References

- [1] R.B. Campbell, Battling tumors with magnetic nanotherapeutics and hyperthermia: turning up the heat, *Nanomedicine* 2 (2007) 649–652.
- [2] Q.A. Pankhurst, N.T.K. Thanh, S.K. Jones, J. Dobson, Progress in applications of magnetic nanoparticles in biomedicine, *J. Phys. D: Appl. Phys.* 42 (2009) 224001.
- [3] P.H. Tran, T.T. Tran, T.V. Vo, B.J. Lee, Promising iron oxide-based magnetic nanoparticles in biomedical engineering, *Arch. Pharmacol. Res.* 35 (2012) 2045–2061.
- [4] L. Li, W. Jiang, K. Luo, H. Song, F. Lan, Y. Wu, Z. Gu, Superparamagnetic iron oxide nanoparticles as MRI contrast agents for non-invasive stem cell labeling and tracking, *Theranostics* 3 (2013) 595–615.
- [5] F. Bähring, F. Schlenk, J. Wotschadlo, N. Buske, T. Liebert, C. Bergemann, T. Heinze, A. Hochhaus, D. Fischer, J.H. Clement, Suitability of viability assays for testing biological effects of coated superparamagnetic nanoparticles, *IEEE Trans. Magn.* 49 (2013) 383–388.
- [6] M. Mahmoudi, S. Laurent, M.A. Shokrgozar, M. Hosseinkhani, Toxicity evaluations of superparamagnetic iron oxide nanoparticles: cell "vision" versus physicochemical properties of nanoparticles, *ACS Nano* 5 (2011) 7263–7276.
- [7] P.H. Hoet, I. Bruske-Hohlfeld, O.V. Salata, Nanoparticles-known and unknown health risks, *J. Nanobiotechnol.* 2 (2004) 12.
- [8] J. Rauch, W. Kolch, M. Mahmoudi, Cell type-specific activation of AKT and ERK signaling pathways by small negatively-charged magnetic nanoparticles, *Sci. Rep.* 2 (2012) 868.
- [9] F. Marano, S. Hussain, F. Rodrigues-Lima, A. Baeza-Squiban, S. Boland, Nanoparticles: molecular targets and cell signalling, *Arch. Toxicol.* 85 (2011) 733–741.
- [10] D.R. Alessi, M. Andjelkovic, B. Caudwell, P. Cron, N. Morrice, P. Cohen, B. A. Hemmings, Mechanism of activation of protein kinase B by insulin and IGF-1, *EMBO J.* 15 (1996) 6541–6551.
- [11] R.Z. Lin, H.Y. Chang, Recent advances in three-dimensional multicellular spheroid culture for biomedical research, *Biotechnol. J.* 3 (2008) 1172–1184.
- [12] J. Lee, G.D. Lilly, R.C. Doty, P. Podsiadlo, N.A. Kotov, In vitro toxicity testing of nanoparticles in 3D cell culture, *Small* 5 (2009) 1213–1221.
- [13] T.T. Goodman, P.L. Olive, S.H. Pun, Increased nanoparticle penetration in collagenase-treated multicellular spheroids, *Int. J. Nanomed.* 2 (2007) 265–274.
- [14] L.G. Griffith, M.A. Swartz, Capturing complex 3D tissue physiology in vitro, *Nat. Rev. Mol. Cell Biol.* 7 (2006) 211–224.
- [15] G. Mehta, A.Y. Hsiao, M. Ingram, G.D. Luker, S. Takayama, Opportunities and challenges for use of tumor spheroids as models to test drug delivery and efficacy, *J. Controlled Release: Off. J. Controlled Release Soc.* 164 (2012) 192–204.
- [16] W. Mueller-Klieser, J.P. Freyer, R.M. Sutherland, Influence of glucose and oxygen supply conditions on the oxygenation of multicellular spheroids, *Br. J. Cancer* 53 (1986) 345–353.
- [17] T.T. Goodman, C.P. Ng, S.H. Pun, 3-D tissue culture systems for the evaluation and optimization of nanoparticle-based drug carriers, *Bioconjug. Chem.* 19 (2008) 1951–1959.
- [18] A. Verma, F. Stellacci, Effect of surface properties on nanoparticle-cell interactions, *Small* 6 (2010) 12–21.
- [19] T.-G. Iversen, T. Skotland, K. Sandvig, Endocytosis and intracellular transport of nanoparticles: Present knowledge and need for future studies, *Nano Today* 6 (2011) 176–185.
- [20] A. Villanueva, M. Canete, A.G. Roca, M. Calero, S. Veintemillas-Verdaguer, C. J. Serna, P. Morales Mdel, R. Miranda, The influence of surface functionalization on the enhanced internalization of magnetic nanoparticles in cancer cells, *Nanotechnology* 20 (2009) 115103.
- [21] L. Treuel, X. Jiang, G.U. Nienhaus, New views on cellular uptake and trafficking of manufactured nanoparticles, *J. R. Soc. Interface* 10 (2013) 20120939.
- [22] M.F. Stins, J. Badger, K. Sik Kim, Bacterial invasion and transcytosis in transfected human brain microvascular endothelial cells, *Microb. Pathog.* 30 (2001) 19–28.
- [23] J.M. Kelm, N.E. Timmins, C.J. Brown, M. Fussenegger, L.K. Nielsen, Method for generation of homogeneous multicellular tumor spheroids applicable to a wide variety of cell types, *Biotechnol. Bioeng.* 83 (2003) 173–180.
- [24] J.M. Atienza, N. Yu, S.L. Kirstein, B. Xi, X. Wang, X. Xu, Y.A. Abassi, Dynamic and label-free cell-based assays using the real-time cell electronic sensing system, *Assay Drug Dev. Technol.* 4 (2006) 597–607.
- [25] M.M. Bradford, A rapid and sensitive method for the quantitation of microgram quantities of protein utilizing the principle of protein-dye binding, *Anal. Biochem.* 72 (1976) 248–254.
- [26] S. Durr, S. Lyer, J. Mann, C. Janko, R. Tietze, E. Schreiber, M. Herrmann, C. Alexiou, Real-time cell analysis of human cancer cell lines after chemotherapy with functionalized magnetic nanoparticles, *Anticancer Res.* 32 (2012) 1983–1989.
- [27] M. Oishi, Y. Nagasaki, N. Nishiyama, K. Itaka, M. Takagi, A. Shimamoto, Y. Furuichi, K. Kataoka, Enhanced growth inhibition of hepatic multicellular tumor spheroids by lactosylated poly(ethylene glycol)-siRNA conjugate formulated in PEGylated polyplexes, *ChemMedChem* 2 (2007) 1290–1297.
- [28] M. Han, Y. Bae, N. Nishiyama, K. Miyata, M. Oba, K. Kataoka, Transfection study using multicellular tumor spheroids for screening non-viral polymeric gene vectors with low cytotoxicity and high transfection efficiencies, *J. Controlled Release: Off. J. Controlled Release Soc.* 121 (2007) 38–48.